the plant journal

SEB SOCIETY FOR EXPERIMENTAL BIOLOGY

The Plant Journal (2022) doi: 10.1111/tpj.15705

High-resolution bin-based linkage mapping uncovers the genetic architecture and heterosis-related loci of plant height in *indica–japonica* derived populations

Weilong Kong[1,2,†], Xiaoxiao Deng[1,†], Jing Yang[1,†], Chenhao Zhang[1], Tong Sun[1], Wenjie Ji[1], Hua Zhong[1], Xiaopeng Fu[3] and Yangsheng Li[1]*

[1]*State Key Laboratory of Hybrid Rice, College of Life Sciences, Wuhan University, Wuhan 430072, China,*

[2]*Shenzhen Branch, Guangdong Laboratory for Lingnan Modern Agriculture, Genome Analysis Laboratory of the Ministry of Agriculture, Agricultural Genomics Institute at Shenzhen, Chinese Academy of Agricultural Sciences, Shenzhen 518120, China, and*

[3]*Key Laboratory of Horticultural Plant Biology, Ministry of Education, College of Horticulture and Forestry Sciences, Huazhong Agricultural University, Wuhan 430070, China*

Received 31 August 2021; revised 5 February 2022; accepted 10 February 2022
*For correspondence (e-mail lysh2001@whu.edu.cn).
†These authors contributed equally to this work.

SUMMARY

Plant height (PH) is an important trait affecting the plant architecture, seed yield, and harvest index. However, the molecular mechanisms underlying PH heterosis remain unclear. In addition, useful PH-related genes must be urgently identified to facilitate ideal plant architecture breeding in rice (*Oryza sativa* L.). In the present study, to explore rice quantitative trait loci (QTLs) and heterosis-related loci of PH in rice, we developed a high-generation (>F_{15}) population of 272 recombinant inbred lines (RIL) from a cross of two elite varieties, Luohui 9 (*in*dica/*xian*) × RPY geng (*japonica*/*geng*), and two testcross hybrid populations derived from the crosses of RILs and two cytoplasmic male sterile lines (YTA [*indica*] and Z7A [*japonica*]). Using deep resequencing data, a high-density genetic map containing 4758 bin markers was constructed, with a total map distance of 2356.41 cM. Finally, 31 PH-related QTLs for different PH component lengths or tiller numbers across five seasons were identified. Two major environment-specific PH QTLs were stably detected in Hainan (*qPH-3.1*) or Hubei (*qPH-5.1*), which have undergone significant functional alterations in rice with changes in geographical environment. Based on comparative genomics, gene function annotation, homolog identification, and existing literature (pioneering studies), candidate genes for multiple QTLs were fine-mapped, and the candidate genes *qPH-3.1* and *qPH-5.1* for PH were further validated using CRISPR–Cas9 gene editing. Specifically, *qPH-3.1* was characterized as a pleiotropic gene, and the *qPH-3.1* knockout line showed reduced PH, delayed heading, a decreased seed setting rate, and increased tiller numbers. Importantly, 10 PH heterosis-related QTLs were identified in the testcross populations, and a better-parent heterosis locus (*qBPH-5.2*) completely covered *qPH-5.1*. Furthermore, the cross results of fixed-genotype RILs verified the dominant effects of *qPH-3.1* and *qPH-5.1*. Together, these findings further our understanding of the genetic mechanisms of PH and offer multiple highly reliable gene targets for breeding rice varieties with ideal architecture and high yield potential in the immediate future.

Keywords: rice, genome resequencing, high-resolution genetic map, plant height, QTL mapping, heterosis-related loci.

INTRODUCTION

Rice (*Oryza sativa* L.) is one of the most important food crops, feeding half of the global population (Song et al., 2021). Asian cultivated rice includes two major types, *indica*/*xian* and *japonica*/*geng* (Wang et al., 2018). Heterosis refers to the phenomenon in which the phenotypes of the hybrid progeny surpass those of their parents in terms of total biomass, growth vigor, and resistance, among other traits, and it is widespread (Birchler et al., 2010). Hybrid rice varieties derived from *indica–indica* crosses produce 20–30% higher yield than inbred rice varieties. This has effectively solved the global food crisis, acquiring

the moniker 'the second green revolution' (Xu et al., 2016). However, the yield increase of *indica–indica* hybrid rice has reached its limit, and the effective utilization of the powerful heterosis between *indica* and *japonica* subspecies has been anticipated as the next important breakthrough to increase rice yield (Huang et al., 2012; Zhang, 2020). Compared with those of intrasubspecies crosses, the offsprings of *indica–japonica* intersubspecies crosses show more evident heterosis owing to the differences in the genetic bases of their agronomic traits (Li et al., 2018; Zhang, 2020). Simultaneously, the *indica–japonica* hybrids have disadvantages, such as super-parental plant height (PH), a low seed setting rate, and prolonged growth duration, which greatly restrict the utilization of intersubspecies heterosis. For instance, increased PH in hybrids increases lodging propensity, resulting in a decrease in rice yield. However, the mechanism of heterosis in rice PH remains unclear. Therefore, the key genes involved in PH and heterotic loci must be urgently explored to solve this dilemma related to the PH of *indica–japonica* intersubspecies hybrids.

The improvement in modern rice varieties can mainly be attributed to plant architecture breeding. Rice plant architecture breeding began with introduction of 'dwarf breeding' in the 1950s. The most successful example of rice improvement is the utilization of the *sd1* gene manipulating the semi-dwarf plant phenotype, which enhanced lodging resistance and improved the harvest index of rice – known as the 'Green Revolution' (Ashikari et al., 2002; Hedden, 2003; Yu et al., 2020). In the 1970s, the yield per unit area of rice was significantly increased by combining plant architecture with heterosis (Virmani, 1994; Yuan, 1994; Yuan & Virnani, 1988). To break through the apparent yield potential barrier, scientists at the International Rice Research Institute proposed specific characteristics of a novel rice ideotype (Janoria, 1989; Khush, 1990; Peng & Cassman, 1994). The modification of PH and tiller number (TN) is now the focus of ideal plant architecture breeding (Li et al., 2012; Springer, 2010; Wang et al., 2017). For instance, a rice multi-functional gene related to PH, panicle shape, and TN was cloned and named *ideal plant architecture 1* (*ipa1*) (Li et al., 2012; Springer. 2010; Wang et al., 2017). At present, the generation of *indica–japonica* hybrids with 'ideal plant architecture' is a fundamental breeding goal to meet the growing demand for food.

To date, intensive efforts have been devoted to dissect the mechanisms of heterosis in *indica–japonica* crosses and clone the major quantitative trait loci (QTLs) related to the 'ideal plant architecture' through QTL mapping or genome-wide association studies. Since the Green Revolution, numerous PH-related genes (over 70) involved in the synthesis, transport, and metabolism of hormones, such as gibberellin, brassinolide, strigolactone, auxin, and abscisic acid, have been cloned (Liu et al., 2018). Nevertheless, very few PH genes can actually be applied in breeding, and the precise functions of these well-known genes are poorly understood (Mahesh et al., 2016; Schatz et al., 2014). For instance, *ipa1* harbors multiple functionally differentiated alleles (Li et al., 2012; Springer, 2010; Wang et al., 2017), while the nine alleles of *sd1* serve different functions, including dwarfing, flooding response, storage durability, and determining panicle architecture (Angira et al., 2019; Biswas et al., 2020; Kuroh et al., 2018; Su et al., 2021). In fact, ideal PH genes still need to be explored through the derived populations of superior rice varieties to provide more selection targets for rice ideal plant architecture breeding.

To explore plant heterosis, conventional breeding components combined with a genetic map have been applied. As a result, several QTLs related to the general combining ability (GCA), special combining ability, better-parent heterosis (BPH), and mid-parental heterosis (MPH) values of various agronomic traits have been reported in different populations (Fan et al., 2019; Li et al., 2016; Xiang et al., 2016; Zhou et al., 2017). These findings of heterosis-related QTLs offer specific candidate targets for the analysis of plant heterosis. However, few heterosis-related genes have been reported to date.

To this end, in the present study, two elite varieties, namely RPY geng (*japonica*) and Luohui 9 (*indica*), which significantly differ in terms of multiple agronomic traits, were selected for the development of recombinant inbred lines (RILs). Luohui 9 (*indica*) exhibits excellent agronomic traits, and RPY geng (*japonica*), carrying the *ipa1* gene, presents an ideal plant architecture (Figure S1). The F_1 progeny of Luohui 9 and RPY geng exhibit obvious heterosis in terms of yield, plant architecture, and resistance, with the heterosis of PH being the most significant among all agronomic traits. Moreover, two testcross populations derived from the crosses of RILs and Z7A (*japonica*) or YTA (*indica*) were used to explore the heterosis of PH. A total of 272 RILs, RPY geng, and Luohui 9 were sequenced to construct a high-density genetic map, and QTLs for PH-related traits and PH heterosis were identified. The genetic effects, gene functions, and heterosis of two unreported environment-specific QTLs, namely *qPH-3.1* and *qPH-5.1*, were characterized. Finally, the aggregation effects of the different alleles of five PH-related QTLs were analyzed in RILs.

RESULTS

Phenotypic variation in PH-related traits among RILs

Here, PH, panicle length (PL), and TN were investigated in Hubei (HB) or Hainan (HN) spanning two to five growing seasons/environments (Figure S3; Figure 1a–c). PH-related traits exhibited significant differences between the HB and HN geographical environments. For instance, the RILs showed higher PH, longer PL, and more tillers in the HB

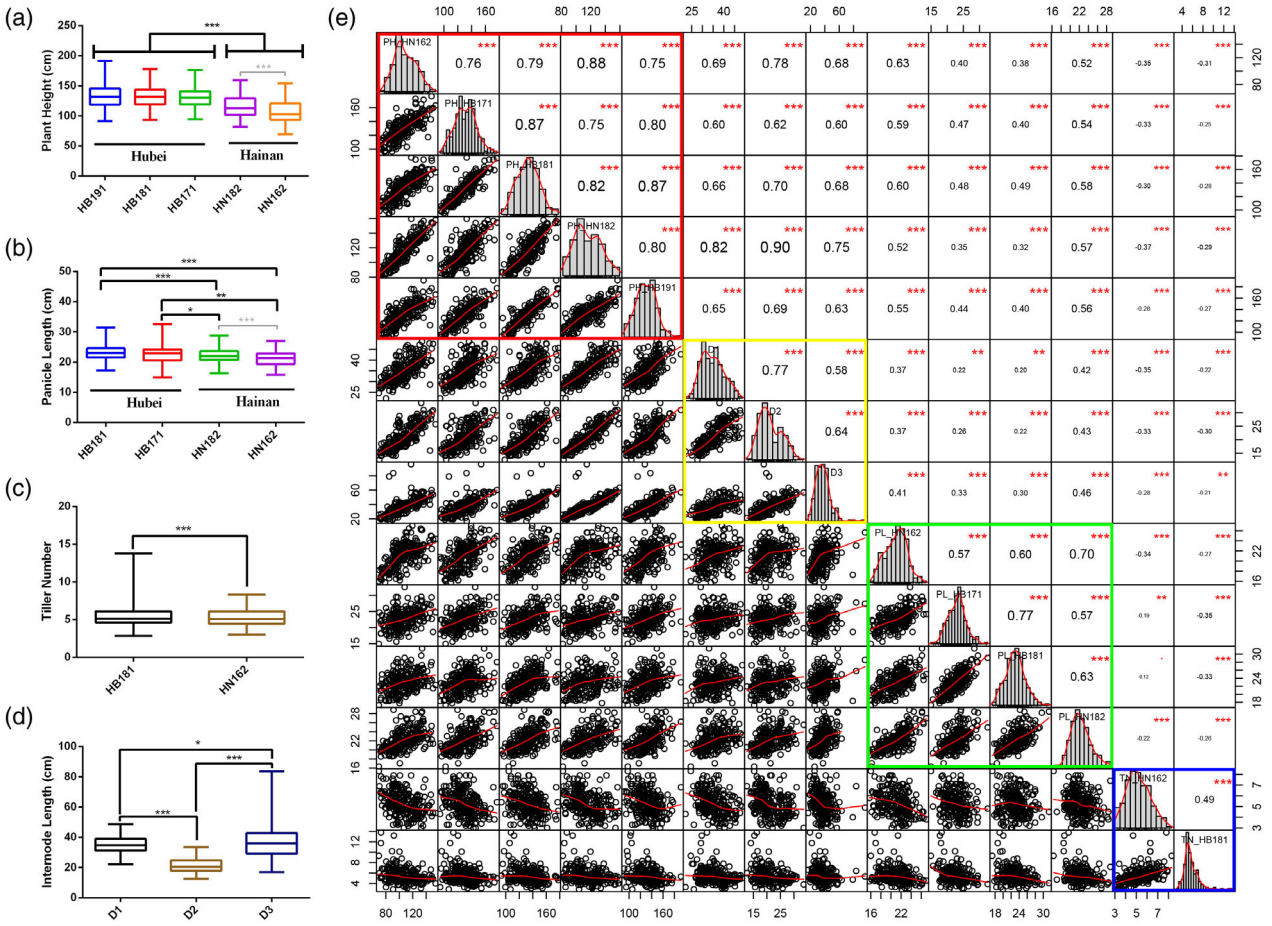

Figure 1. The plant height-related traits of RILs in Hubei (HB) and Hainan (HN). (a–c) Boxplots of plant height, panicle length, and tiller number in HB and HN over multiple years, namely, F_{11} in HN (HN162), F_{12} in HB (HB171), F_{14} in HB (HB181), F_{15} in HN (HN182), and F_{16} in HB (HB191). The gray connecting line represents the difference of this trait in different years in the same province. The black connecting line represents the difference of this trait between HB and HN. (d) Boxplots of different internode lengths of RILs in HN182. (e) Histogram, regression statistics, and Pearson correlation coefficient of plant height (PH), panicle length (PL), tiller number (TN), the uppermost internode length (D1), the penultimate internode length (D2), and the remaining internode length (D3) in HB and HN over multiple seasons. The red box is the plant height; the yellow box is the internode length; the green box is the panicle length; the blue box is the number of tillers. $*P < 0.05$, $**P < 0.01$, $***P < 0.001$, Student's *t*-test.

environment than in HN (Figure 1a–c). In addition, there was no significant difference in PH and PL of RILs among HB191, HB181, and HB171 (Figure 1a,b). To explore PH components, the PH in HN182 was further divided into four components: PL, uppermost internode length (IL) (D1), penultimate IL (D2), and remaining IL (D3) (Figure S3b; Figure 1d). Of them, D3 showed a higher coefficient of variation relative to D1 and D2 (Figure 1d; Table S1). TN and IL showed greater variations than PH and PL, suggesting that TN and IL are more sensitive to changes in the geographical environment (Table S1).

PH-related traits all showed normal distributions, which implied that PH-related traits were typical quantitative traits involving multiple genes (Figure 1e). The correlation coefficient showed that PH, PL, IL, and TN were significantly positively or negatively correlated in all environments (Figure 1e).

Bin-based genetic map and PH-related QTLs

A total of 396.31 Gb of clean data from the 272 RILs, with an average depth of 3.33× for the Nipponbare genome on average for each RIL, was obtained. In total, 1 339 300 high-quality single-nucleotide polymorphisms (SNPs) (>4× depth) were selected and divided into 12 linkage groups (LDs) containing 4758 bins, with a total genetic map distance of 2356.41 cM, using HighMap (Liu et al., 2014). The average distance between two adjacent bin markers was <0.5 cM (Figure 2a). This high-density genetic map showed an excellent correlation with the Nipponbare physical map (Figure 2b).

Eight PH-related QTLs were identified (Figure 2c; Table S2). Among these, the overlap interval (38 302 079–38 693 562, only 0.39 Mb) of three QTLs (*qPH-1.1*, *qPH-1.2*, and *qPH-1.3*) was named *qPH-1*, which harbored the *sd1*

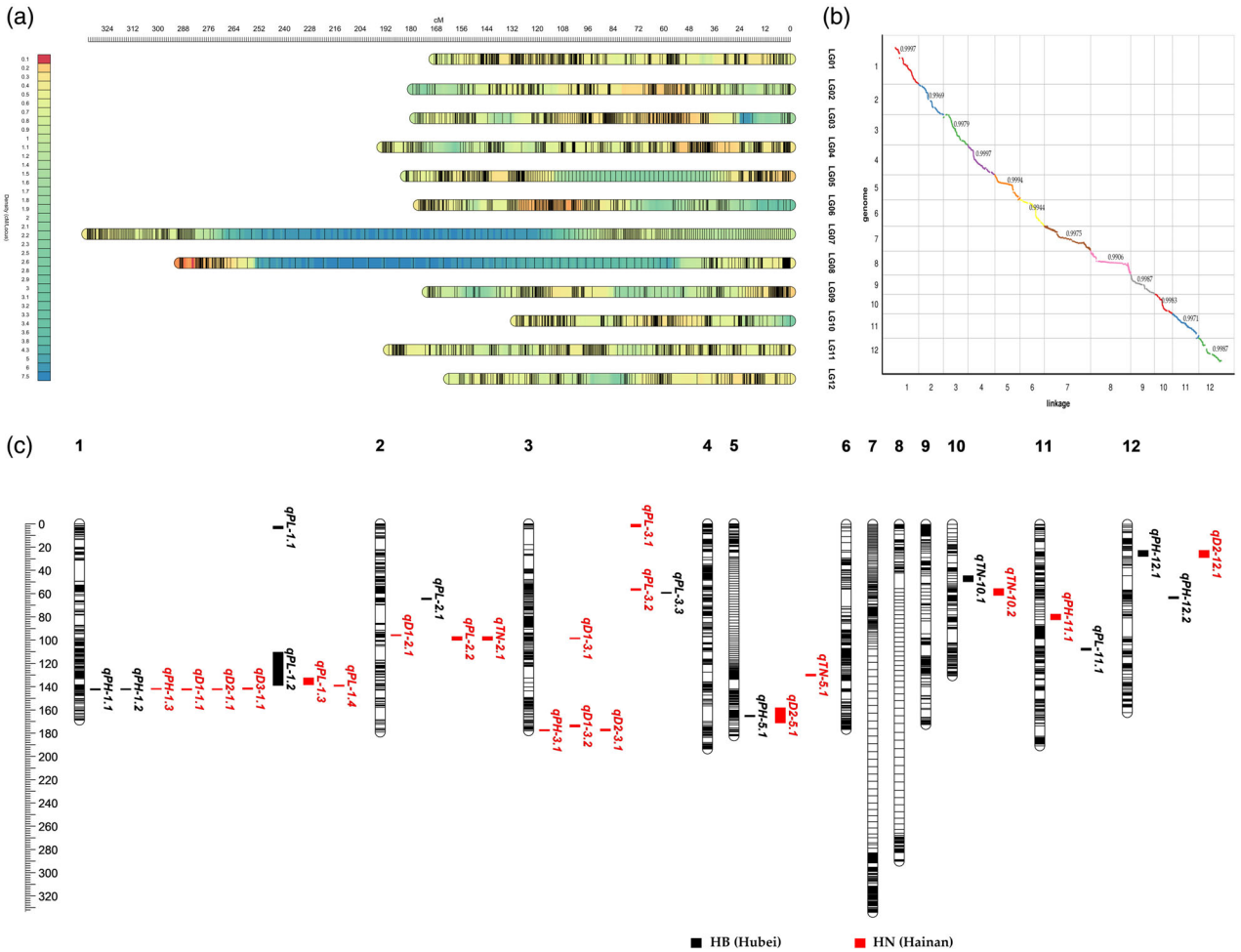

Figure 2. Bin-based genetic map and QTLs of plant height-related traits. (a) The density of genetic bin markers among the linkage groups. (b) Correlation between genetic map and physical map (Nipponbare, MSU V7.0). (c) QTLs of plant height (PH), tiller number (TN), internode length (IL), and panicle length (PL) traits in linkage groups visualized through Mapchart software.

gene and was repeatedly detected every year, explaining 27.21–54.73% of the phenotypic variation. Importantly, two HN environment-specific QTLs, namely *qPH-3.1* and *qPH-11.1*, and three HB environment-specific QTLs, namely *qPH-5.1*, *qPH-12.1*, and *qPH-12.2*, were repeatedly discovered. Of these, *qPH-3.1* and *qPH-5.1* were adopted as the major environment-specific QTLs with high limit of detection (LOD) values (4.10–10.42), explaining 7.88–18.83% of the phenotypic variation.

Interestingly, the major QTLs related to IL and PH, namely, *qD1-1.1* and *qPH-1.1*, *qD2-1.1* and *qPH-1.2*, and *qD3-1.1* and *qPH-1.3*, completely matched (Figure 2c; Table S2). These results suggest that *qPH-1*, as a major QTL for both IL and PH, likely affects PH by manipulating IL. In addition, 10 QTLs related to PL were detected on chromosomes 1, 2, 3, and 11. Remarkably, multiple QTLs related to PL were distributed in tandem or in clusters. For instance, *qPL-3.2* and *qPL-3.3* carried a 0.315-Mb intersection, and *qPL-1.2*, *qPL-1.3*, and *qPL-1.4* were distributed in clusters (Figure 2c). In addition, four QTLs related to TN, including three HN environment-specific QTLs (*qTN-2.1*, *qTN-5.1*, and *qTN-10.2*) and one HB environment-specific QTL (*qTN-10.1*), were detected (Figure 2c; Table S2).

Known QTL genes affecting the PH-related traits of RILs

In the present study, 306 known PH-related genes were retrieved from RiceData (https://www.ricedata.cn/), NCBI (https://www.ncbi.nlm.nih.gov/), Google Scholar (http://scholar.goole.com), and CNKI (https://www.cnki.net/), including 221, 27, 22, and 106 genes for PH, IL, PL, and TN, respectively (Table S3; Figure S4). Seven known genes were detected in the corresponding trait QTLs (Table S4), such as *sd1* in *qPH-1*, *OsCIGR* in *qPH-1.3*, *Ostrxm* in *qPH-12.1*, *PSRK2* in *qD1-1.1* and *qD2-1.1*, *SBI* and *OsCOLE1* in *qD2-5.1*, and *OsPLIM2a* in *qTN-2.1*. Six of these (excluding *OsPLIM2a*) differed in terms of protein sequence between Luohui 9 and RPY geng (Table S5).

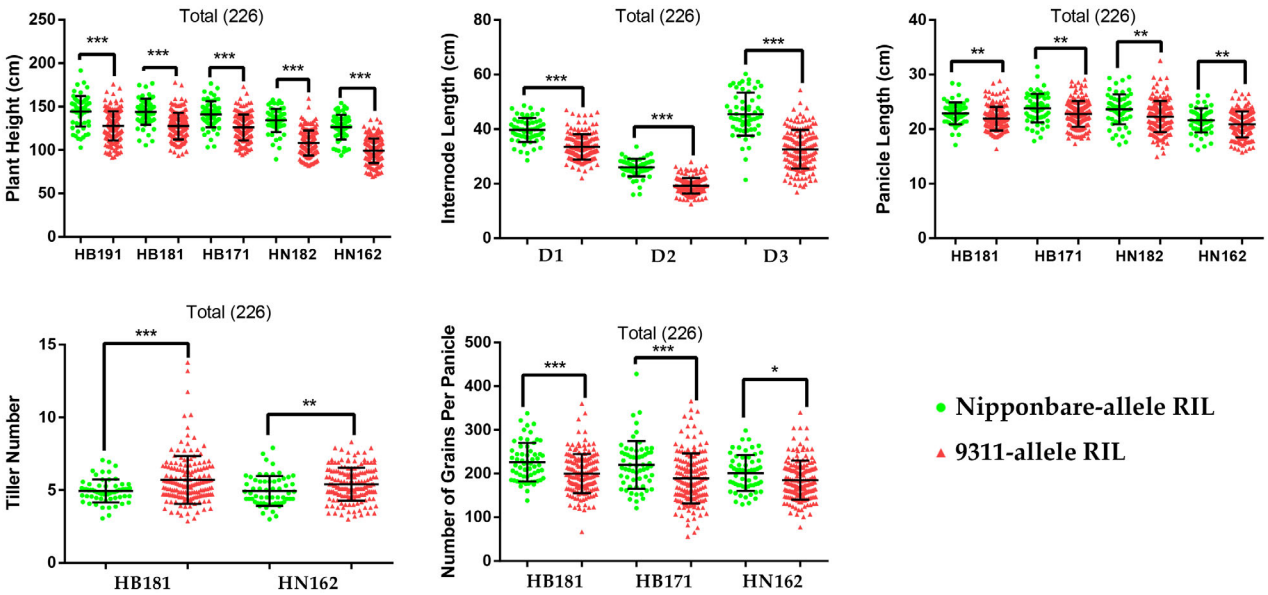

Figure 3. Trait comparison of RILs with different *sd1* alleles: plant height, internode length, panicle length, tiller number, and number of grains per panicle, in multiple environments. *$P < 0.05$, **$P < 0.01$, ***$P < 0.001$, Student's *t*-test. RILs with the Nipponbare allele and the 9311 allele of the *sd1* gene are marked by green dots and red triangles in point clouds, respectively. The *x*-axis represents the environments of each pair of point clouds, and the abbreviations of the environments (HB191, HB181, HB171, HN182, and HN162) and internode lengths (D1, D2, and D3) are consistent with Figure 1. Total (226) represents valid RILs for the *sd1* locus (homozygous Nipponbare allele or homozygous 9311 allele); heterozygous RILs and RILs for which genotyping failed (NA) are not counted.

The *sd1* gene in *qPH-1* was identified in at least nine multiple alleles (Figure S5a). RPY geng and Luohui 9 carried the Nipponbare allele and the 9311 allele, respectively. Compared with the Nipponbare allele, the 9311 allele harbors four nucleotide mutations, of which three are non-synonymous and the fourth leads to early termination of translation of the sd1 protein (Figure S5b,c). Furthermore, PH and IL differed between RILs carrying the Nipponbare allele and the 9311 allele (Figure 3). As such, PH and IL in RILs carrying the Nipponbare allele were higher than those in RILs carrying the 9311 allele. Notably, the RILs carrying these two different alleles also significantly differed in terms of PL, TN, and grain number per panicle (GNP). These results indicate that *sd1* (*qPH-1*) is a pleiotropic gene for PH, IL, PL, TN, and GNP. The findings refine our understanding of the effects of *sd1*.

Similarly, PH, IL, PL, TN, and GNP significantly differed between RILs carrying the RPY geng and Luohui 9 alleles of *OsCIGR* in *qPH-1.3* (Figure S6). Moreover, the *Ostrxm* gene in *qPH-12.1* only affected PH in the HB environment (Figure S7a,c). Interestingly, the effect of *Ostrxm* on IL was strongly influenced by the *sd1* alleles. Only in the presence of the Luohui 9 *sd1* allele (*Mosd1*), RILs carrying the different *Ostrxm* alleles showed significant differences in D1 and D2 (Figure S7b,d). Furthermore, RILs carrying the different *PSRK2* (in *qD1-1.1* and *qD2-1.1*; Figure S8a) alleles significantly differed in terms of PH, IL, PL, TN, and GNP (Figure S8b–f). In *qD2-5.1*, *SBI* and *OsCOLE1* were located at block 148192 and block 148452, respectively (Figure S9a, d). PH and IL were significantly different between RILs carrying different *SBI* alleles (Figure S9b,c) but not between those carrying different *OsCOLE1* alleles (Figure S9e). These findings indicate that *SBI* is the candidate gene in *qD2-5.1*, which affects total PH by manipulating IL. Overall, the known genes play pivotal roles in PH of RILs and may serve unreported functions.

Fine mapping of QTLs for PH-related traits

Based on the homolog identification of 306 known PH-related genes and parental protein sequence alignment of the homologous pairs, a total of 78 candidate genes were identified within the detected QTLs (Figure S10b; Table S6). Of these, *qPH-3.1*/*qD2-3.1*, *qPH-11.1*, *qD1-3.2*, and *qPL-1.4* only harbored one candidate gene each, while *qPH-12.1* and *qTN-5.1* harbored two candidate genes each. The number of genes within the other QTLs was below 15 (Figure S10b).

Several QTLs with few candidate genes were analyzed. For instance, *LOC_Os03g64415* (the homolog of *BC12* and *DBS1*) was the only candidate gene in *qPH-3.1* and *qD2-3.1*, and it was located at the end of chromosome 3. We extracted *LOC_Os03g64415* and its five upstream genes for collinearity analysis. The five upstream genes showed excellent collinearity relationships between RPY geng and Luohui 9, but the DNA sequences of parental *LOC_Os03g64415* genes were different (Figure 4a,b). PH and IL in RILs carrying different *LOC_Os03g64415* alleles were significantly different among some years (Figure S11a,b). Considering that *sd1* is the major gene

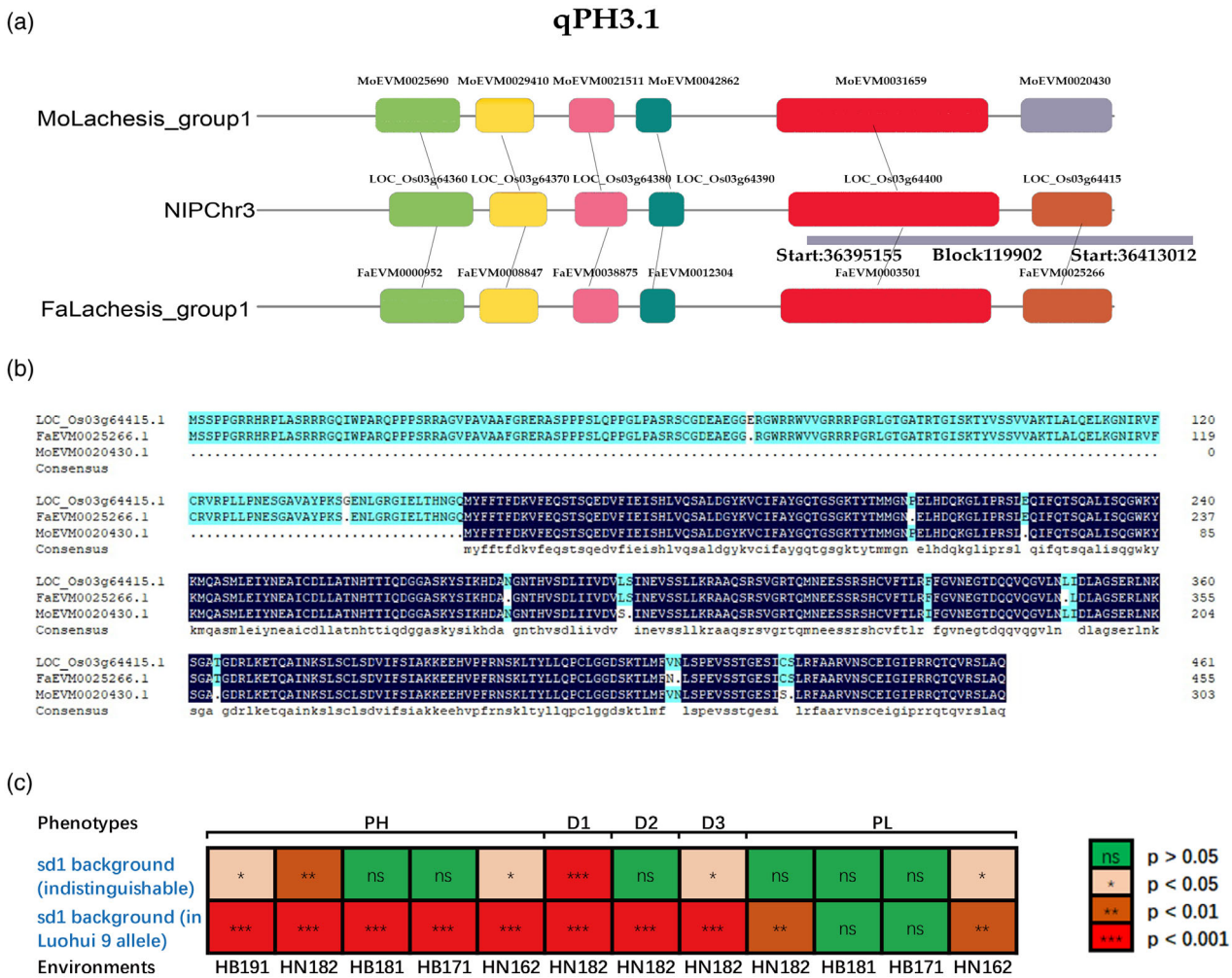

Figure 4. Analysis of candidate genes in *qPH-3.1*. (a) Collinearity analysis of Luohui 9, Nipponbare, and RPY geng (upstream five genes + *LOC_Os03g64415*). (b) Sequence alignment of *LOC_Os03g64415* sequences from Nipponbare, RPY geng, and Luohui 9. (c) Epistasis between *sd1* and *LOC_Os03g64415*. Each box represents the significance of the difference in plant height of different allelic RILs of *LOC_Os03g64415* under different environments or different internode lengths.

affecting PH, its different genetic backgrounds may conceal the effects of other genes on PH-related traits. We therefore compared the PH-related traits of 161 RILs carrying different *LOC_Os03g64415* alleles under the *sd1* Luohui 9 allele background to circumvent the potential epistatic effect of *sd1* on *LOC_Os03g64415*. As expected, PH and IL in RILs carrying different *LOC_Os03g64415* alleles were significantly different among all years (Figure S11d,e). These results indicated that *LOC_Os03g64415* is a candidate gene for PH and may affect PH by manipulating IL but not PL (Figure S11c,f). Moreover, the function of this gene is greatly affected by the genetic background of the *sd1* gene (Figure 4c). In the Luohui 9 allele of the *sd1* background, the differences in RILs carrying different alleles of *LOC_Os03g64415* became more significant relative to the case without considering the *sd1* background (Figure 4c). This result implied epistasis between *sd1* and *LOC_Os03g64415*.

LOC_Os05g45180, a homolog of *OsIAGLU*, was a peak marker for *qPH-5.1* (Figure S12a). RILs carrying different *LOC_Os05g45180* alleles showed significantly different PH and IL (Figure S12b,c). This gene was predominantly expressed in IL and shoot tissues (Figures S12d and S13). Therefore, *LOC_Os05g45180* is a candidate gene for *qPH-5.1*.

LOC_Os11g19060, a homolog of *SMOS1*, was the only candidate for *qPH-11.1*, which was also affected by *sd1* like *qPH-3.1*. As such, PH and PL in RILs carrying different *LOC_Os11g19060* alleles were significantly different in the RILs with the *sd1* Luohui 9 allele background (Figure S14).

Finally, *LOC_Os01g64590*, a homolog of *SP3*, was the only candidate for *qPL-1.4*. In addition to PL, this gene affected PH, IL, TN, and GNP (Figure S15a–f). Notably, *LOC_Os01g64590* was highly expressed in panicle tissue at multiple time points, indicating its potential function in panicles (Figure S15g). Similarly, two candidate genes,

both homologs of *OsEATB*, were characterized in *qTN-5.1* (Figure S16).

Functional characterization of the candidate genes for *qPH-3.1* and *qPH-5.1*

We confirmed the functions of the candidate genes for *qPH-5.1* and *qPH-3.1* through CRISPR–Cas9 gene editing (Figure 5a). Three CRISPR–Cas9-mediated mutation lines of *qPH-3.1* were obtained, including two 1-bp insertion lines and a 3-bp deletion line. A 1-bp insertion line, a 3-bp deletion line, and a 84-bp deletion line of *qPH-5.1* were developed (Figure S17). PH, IL (D2 and D3), and PL of the *qph-5.1* and *qph-3.1* lines were significantly reduced (Figure 5b–e). Specifically, the magnitude of reduction in PH, IL, and PL was greater in *qph-3.1* than in *qph-5.1*. Moreover, the PH of *qph-3.1* (57 cm) was approximately half of that of the wild type (WT; 98 cm) and *qph-5.1* (90 cm). Importantly, *qph-3.1* showed a marked prolongation of the growth period (>15 days) and a severe decrease in the seed setting rate (close to zero), and the main tiller became difficult to distinguish; instead, *qph3-1* produced more tillers than the WT and *qph-5.1* (Figure 5b,d,e). These results indicate that *qPH-5.1* and *qPH-3.1* affect rice PH and that *qPH-3.1* is a pleiotropic gene associated with PH, growth period, fertility, and tillering.

Heterosis-related QTLs for PH

We detected two QTLs for GCA, four QTLs for MPH, and four QTLs for BPH (Figure S18). Of these, five known PH-related genes were included in heterosis-related QTLs, namely *sps1* in *qMPH-1.1*; *OsPIN2*, *AP01*, and *OsPLS1* in *qMPH-6.1*; and *SBI* in *qBPH-5.1*. Three of the 10 heterosis-related QTLs overlapped with rice PH-related QTLs: *qBPH-3.1* overlapped with *qPL-3.2*; *qBPH-5.1* and *qBPH-5.2* were nested within *qD2-5*; and *qBPH-5.2* was covered by *qPH-5.1* (Figure S18).

Understanding the genetic effects of environment-specific PH QTLs, *qPH-3.1* and *qPH-5.1*, will help to apply them in breeding. Since the high-generation RILs are all homozygous lines, the dominance effect of each QTL cannot be estimated in linkage mapping (Li et al., 2015). To examine dominance effects of *qPH-3.1* and *qPH-5.1*, we made hybrid crosses between seven RILs (the genotypes of these seven RILs are provided in Table S7). For analysis of the dominance effects of *qPH-3.1*, the remaining four PH QTLs (*qPH1*, *qPH-5.1*, *qPH-11.1*, and *qPH-11.1*) alleles must be the same in the two selected RILs for minimizing background effects, but the *qPH-3.1* alleles were opposite. The dominance effect of *qPH-3.1* was repeatedly verified using two pairs of RILs following the reciprocal crossing scheme (Figure 6a,b). The same cross design was used for the dominant effect analysis of *qPH-5.1* (Figure 6c,d). For different alleles of *qPH-3.1*, the tall allele shows complete dominance over the short allele (significant differences in PH between AA/Aa and aa; no difference between AA and Aa) (Figure 6a,b). Similarly, *qPH-5.1* showed complete dominance on PH (Figure 6c,d).

QTL aggregation as reference for PH precision breeding

In the present study, both *qPH-3.1* and *qPH-11.1* were affected by the background of the *qPH-1* (*sd1*) gene, and both *qPH-3.1* and *qPH-5.1* were environment-specific. These QTLs are most likely not functionally independent and combinations of their different alleles may produce different rice PHs. Thus, we explored the allele combinations of *qPH-1* (*sd1*), *qPH-3.1* (*LOC_Os03g64415*), *qPH-5.1* (*LOC_Os05g45180*), *qPH-11.1* (*LOC_Os11g19060*), and *qPH-12.1* (*Ostrxm*) in RILs, and totally found 38 allelic combinations (P1–P38). These allelic combinations were numbered from the largest to smallest (P1–P10) containing the number of RILs, and allelic combinations with fewer than seven RILs were uniformly marked as 'other' (Table S8). The average PHs in RILs carrying different allelic combinations were evidently different in one environment but these differences remained relatively stable over the years (Figure 7a–e). Notably, the HN environment made the difference of some allelic combination pairs significant compared to the HB environment, such as P6 and P4 as well as P6 and P5 (Figure 7d,e versus Figure 7a–c). The differences between most allelic combination pairs were very stable (Figure 7f). For instance, RILs carrying P4, P5, and P9 showed the highest PH, whereas those carrying P3 and P8 showed the lowest PH in environments (Table S8; Figure 7a–e). In addition, PH and the number of QTL tall alleles were positively correlated (Table S9). These results suggested that rice lines with the expected heights can be accurately designed by aggregating different alleles of five PH QTLs.

DISCUSSION

PH component classification can detect more QTLs and help to reveal their underlying mechanisms

Many previous studies only focused on a specific key trait but ignored the changes in other related traits. In fact, different agronomic traits, particularly those related to PH, are obviously interlinked, as evidenced by the correlation patterns observed in the present study (Figure 1). Rice PH is a complex trait affected by multiple genes and constitutes multiple components, such as PL and IL. Some genes may affect multiple PH components, such as *sd1* (Spielmeyer et al., 2002), while other individual genes may affect specific PH components, such as *dep1*, which is responsible for PL (Fumio et al., 2011). Compared with the QTL analysis of the total PH alone, the QTL analysis of PH-related components can effectively identify more QTLs as well as loci for specific PH components that are likely to be masked by the total PH. Benefiting from the division of PH

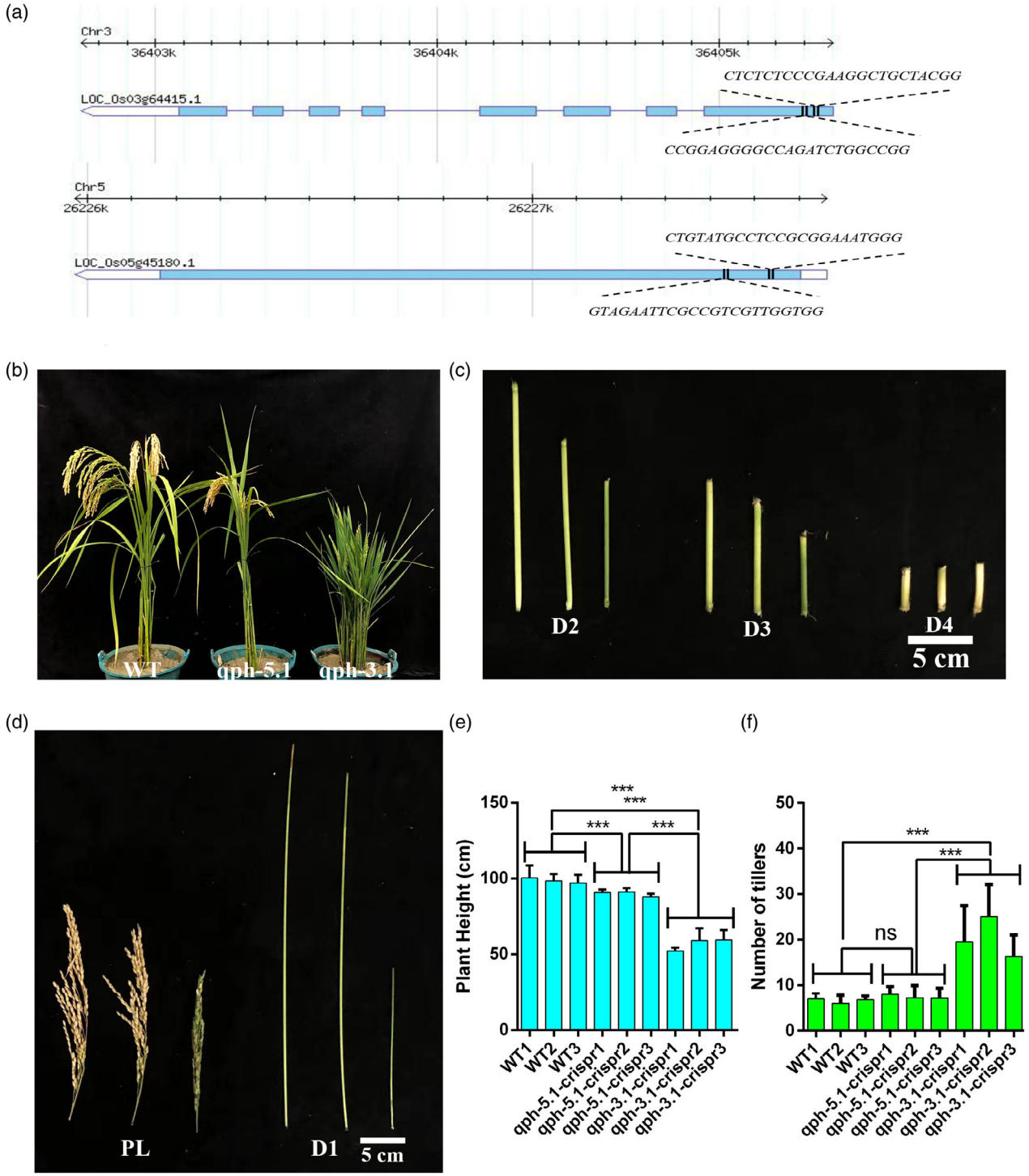

Figure 5. CRISPR–Cas9 gene editing of *qPH-3.1* and *qPH-5.1*. (a) Schematic diagram of the genomic region and the sgRNA target site of *qPH-3.1* and *qPH-5.1*. (b) WT, *qph-5.1* mutant, and *qph-3.1* mutant plants. (c) From left to right, internode length of WT, *qph-5.1* mutant, and *qph-3.1* mutant plants. D2, D3, and D4 mean different internode length components. (d) Panicle length and D1 of WT, *qph-5.1* mutant, and *qph-3.1* mutant plants. (e) Plant height of WT, *qph-5.1* mutant, and *qph-3.1* mutant plants. (f) Tiller number of WT, *qph-5.1* mutant, and *qph-3.1* mutant plants. In (e) and (f), ns indicates non-significant, ***$P < 0.001$, Student's *t*-test.

components in sorghum (*Sorghum bicolor*), Li et al. (2015) discovered a PH-related QTL, *qPT7.1*, placed near the major PH QTL, *Dw3*; *qPT7.1* is repulsively linked to *Dw3* and could not have been detected in the QTL analysis of total PH. Meanwhile, the comparative analysis of various PH components between RILs with opposite alleles can

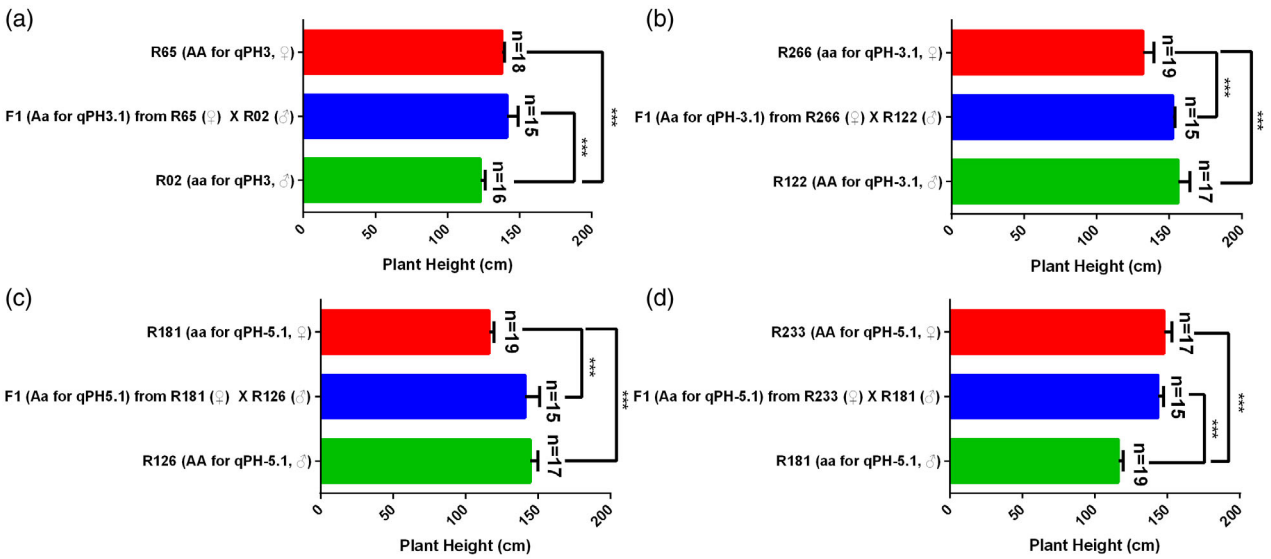

Figure 6. Plant height of parental lines and corresponding F_1 hybrids. (a, b) The tall allele (AA) shows complete dominance over the short allele (aa) of *qPH-3.1* under positive and negative crossing verification. (c, d) The tall allele (AA) shows complete dominance over the short allele (aa) of *qPH-5.1* under reciprocal crossing verification. In each panel, top, middle, and bottom columns are the pollen parent, the seed parent, and the F_1 hybrid. ***$P < 0.001$, Student's *t*-test. R02, R65, R122, R266, R126, R181, and R233 represent the numbers of RILs selected for hybrid crosses in this study; the genotypes of these seven RILs are provided in Table S7.

unveil specific QTLs that affect the total PH through affecting specific PH components. For instance, *sd1*, *qPH-3.1*, and *qPH-5.1* all mediated PH by influencing IL, while *qPH-11.1* affected PH by manipulating PL. Importantly, the results of our comparative analysis among RILs with different alleles broadened the functional understanding of several known genes. Specifically, we noted that known genes such as *sd1*, *OsCIGR*, and *PSRK2* affect not only PH but also multiple PH-related traits. For instance, *sd1*, as an important semi-dwarf gene, can significantly reduce PH and improve lodging resistance and yield per unit area of rice (Spielmeyer et al., 2002). Recently, *sd1* was proven to play important roles in panicle architecture, flooding response, and storage durability (Biswas et al., 2020; Kuroh et al., 2018; Spielmeyer et al., 2002; Su et al., 2021). Our results showed that in addition to these known functions, *sd1* may simultaneously affect PL, TN, and GNP. Overall, component analysis reduced the complexity of PH, allowing a greater QTL resolution. This approach will serve as a useful tool for the functional analyses of other complex QTLs in plants.

High-density bin-based linkage analysis combined with homolog identification allows for the fine mapping of QTLs

Previous QTL studies on rice were conducted using limited restriction fragment length polymorphism and simple-sequence repeat markers. Typically, the physical distance of QTLs ranges between 4 and 10 Mb, harboring numerous genes due to the sparse marker density. In the present study, 58.06% (18/31) of the detected QTLs showed a physical distance of <100 kb, whereas 12.90% (4/31) of the detected QTLs spanned over <10 kb and contained single-digit coding genes. For instance, *qPH-3.1* was only 0.03 Mb and contained seven genes. Such an extremely narrow interval allowed us to efficiently fine map this QTL through the comparative analysis of parental genomes. In addition, the homolog analysis of known genes integrated in the fine mapping of the detected QTLs reduced the number of candidate genes to one or two. The candidate genes in *qPH-3.1*/*qD2-3.1* (only one gene), *qPH-11.1* (one gene), *qPL-1.4* (one gene), and *qTN-5.1* (two genes) were further validated through genotyping and expression analyses. It is worth mentioning that reliance on homology analysis may lead to the omission of some unreported candidate genes, because the homologous sequences of these unreported candidate genes have not been proved to be related to PH, which led to deletion in our query sequences. This may also be one of the possible reasons why we have not found candidate genes in some of our QTLs, and the discovery of these unreported candidate genes may have to rely on the fine mapping population. This also warns us that the homolog analysis may fail for some traits without *a priori* known genes. However, for most traits in rice, high-density bin-based linkage analysis combined with homolog identification is an efficient and time-saving method.

Environment-specific QTLs play important roles in rice PH

Rice PH is affected by the genetic background and ecological environment. In the present study, we identified two

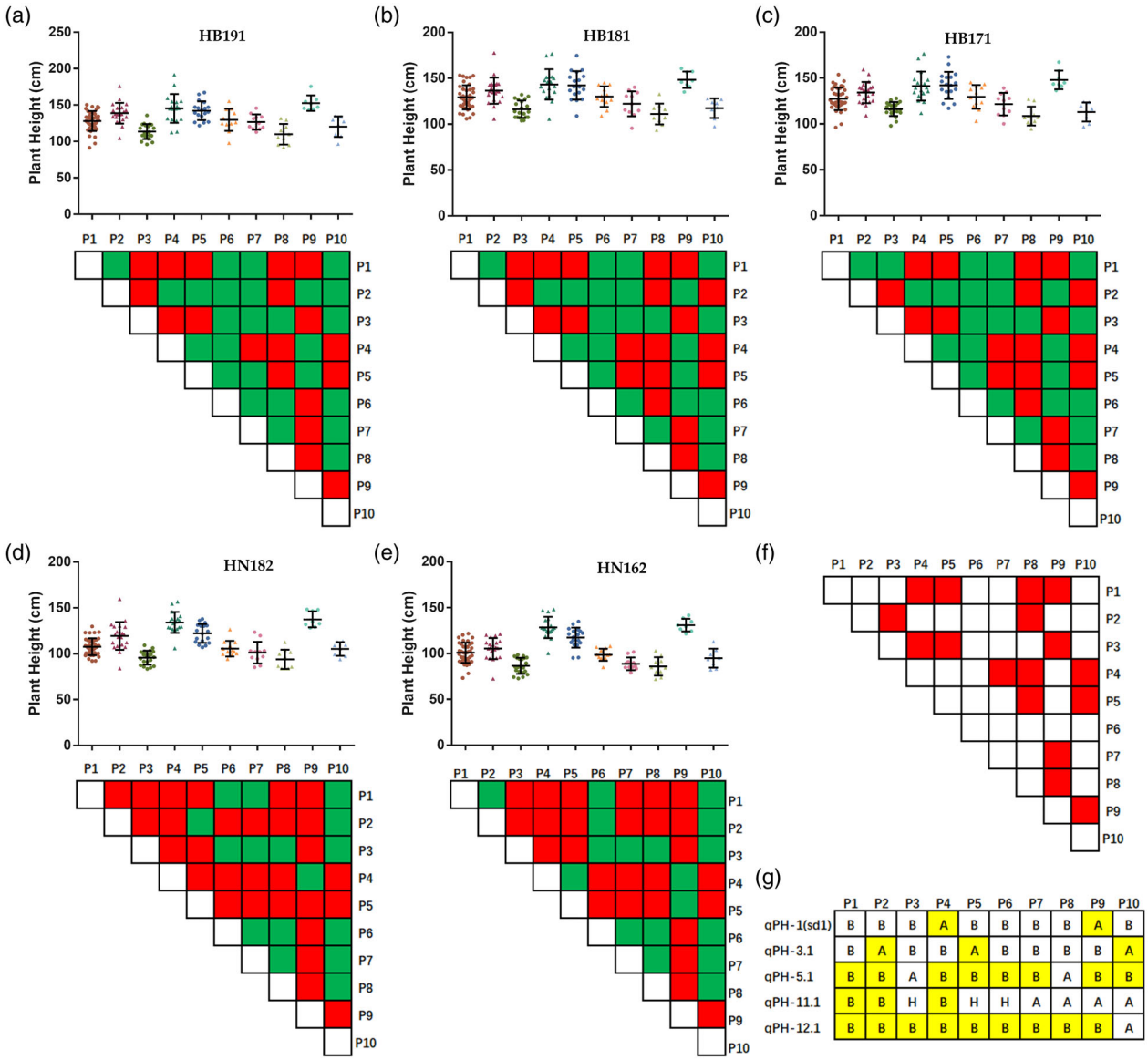

Figure 7. Plant heights of different allelic combinations of five identified plant height QTLs. (a–e) Upper panel: Plant height of P1–P10 in five environments (HB191, HB181, HB171, HN182, and HN162; for abbreviations see Figure 1). Lower panel: Heatmap of significant differences among P1–P10. The green square indicates that there is no significant difference between the two allelic combinations, and red indicates that there is a significant difference ($P < 0.05$), as determined by one-way analysis of variance (ANOVA). (f) Allelic combination pairs with significant differences ($P < 0.05$) in five environments are highlighted with red squares. (g) The genotypes including *qPH-1*, *qPH-3.1*, *qPH-5.1*, *qPH-11.1*, and *qPH-12.1* of 10 allelic combinations (P1–P10). The allele with a yellow background represents the tall allele for each QTL. The 'A' alleles represent RPY geng alleles and 'B' alleles represent Luohui 9 alleles. In (a–e), one-way ANOVA was performed with GraphPad Prism software (https://www.graphpad.com/scientific-software/prism/) with ordinary one-way ANOVA and Bonferroni's multiple comparisons, with a single pooled variance.

environment-specific PH-related QTLs and found that environment affects the significance of differences in allelic combination pairs. Several genes related to yield or heading date identified in previous studies are also strongly affected by environmental factors. For example, *Hd3a* overexpression promoted flowering under short-day conditions, while *Hd3a* suppression delayed flowering under long-day conditions. Another study reported that *Ghd7* was affected by the photoperiod and circadian rhythm and the specific daytime expression of *Ghd7* gene under long-day conditions potently inhibited the heading date gene in rice, resulting in a delayed heading phenotype. Moreover, Li et al. (2018) reported that *Gn1a*, *SDG708*, *SD1*, *GW5*, *PHYB*, and *DEP1* functions were affected by the geographical environment. Our results suggested that the geographical environment can affect rice PH through specific QTLs, and the effects of these QTLs are strongly affected by the geographical environment. This phenomenon may be

closely linked to light- and temperature-related genes. In the present study, the natural conditions, such as light and temperature, were markedly different between Hainan and Hubei. However, the specific mechanisms and genes involved remain to be explored.

qPH-3.1 is an important pleiotropic gene

qPH-3.1 harbored only a homolog gene (*LOC_Os03g64415*) of the known PH-related genes, which encodes a kinesin domain-containing protein, and this gene was affected by the background of the *sd1* gene. We speculated that *LOC_Os03g64415* affects the total PH of rice by manipulating IL and that it is likely involved in the gibberellin pathway. Our hypothesis is supported by the functions of the homolog, *BC12*. In particular, *BC12* is a pleiotropic gene affecting IL, PH, PL, and TN in rice. *BC12* is involved in the gibberellin pathway, and the defective phenotype of the *bc12* mutants whose PH, IL, and PL were significantly reduced could be rescued through exogenous gibberellin application (Li et al., 2011; Yu et al., 2016; Zhang et al., 2010). Another gene in the same gene family, *DBS1*, also affects the total PH (Sazuka & Kawai, 2005). Specifically, the *dbs1* mutant exhibits severe defects in shoot and root growth, and the defective phenotypic cannot be rescued even with gibberellin treatment (Sazuka & Kawai, 2005). Fang et al. (2018) cloned the *stem dwarf 1* (*std1*) gene and found that the mutant of this gene showed altered IL, exhibiting an extreme dwarf phenotype. Based on these reports, *LOC_Os03g64415* may share partial functional redundancy with *BC12*, and the members of this family have undergone significant functional differentiation.

Finally, using CRISPR–Cas9 gene editing, we confirmed that *qPH-3.1* is an important pleiotropic gene related to PH, growth, seed setting, and tillering. These results imply that *qPH-3.1* is closely related to the normal growth, development, and yield of rice. Screening natural populations for the optimal alleles of *qPH-3.1* will pave the way for ideal plant architecture breeding of rice.

EXPERIMENTAL PROCEDURES

Plant material and population construction

In the present study, a high-generation population of 272 RILs was developed from a cross between Luohui 9 and RPY geng using the single-seed descendant method since 2011 (Figure S2).

To detect PH heterosis-related QTLs, two testcross populations (Z7A-TCF1 and YTA-TCF1) were developed by crossing the RILs (F_{14}) with Z7A or YTA (Figure S2). All crosses were performed in the spring of 2019 in the Hybrid Rice Experimental Base of Wuhan University in Lingshui City (18°N, 110°E), Hainan Province.

Experimental design

In 2017–2019, the RILs (F_{11}–F_{16}) and parents were planted in the experimental field of the Ezhou Experimental Base of Wuhan University/Breeding Experimental Base of Wuhan University, Tianyuan Co., Ltd. in Hannan District (30°N, 114°E), Wuhan City, Hubei Province (from mid-May to October) or the Hybrid Rice Experimental Base of Wuhan University in Lingshui City (18°N, 110°E), Hainan Province (from December to April of the next year): F_{11} in HN (abbreviated as HN162), F_{12} in HB (Ezhou, abbreviated as HB171), F_{14} in HB (Ezhou, abbreviated as HB181), F_{15} in HN (abbreviated as HN182), and F_{16} in HB (Hannan, abbreviated as HB191) (Figure S3a).

In each season, a randomized complete block design in the same field was carried out for RILs and no less than 15 replications for parents were used to evaluate the overall uniformity of the experimental field. Sixty plants of each line from 272 RILs or parents were planted in six rows with 10 plants per row, where the spacing of plants and lines was 13.3 cm × 20 cm and 30 cm, respectively. The same field experimental design was used for the Z7A-TCF1, YTA-TCF1, and RIL populations at the Breeding station in Hannan District, Wuhan City, Hubei Province, China, in 2019. All plants were under standard agricultural planting management.

RIL resequencing and genetic map construction

Young leaves of the 272 RILs (F_{10} or F_{11}) were collected in liquid nitrogen. The genomic DNA of the collected leaves was extracted using the modified CTAB method (Attitalla, 2011) and then sequenced on an Illumina HiSeq^{TM} 2500 (Illumina, Delaware, DE, USA) platform using the paired-end 150 bp method. Raw read data were filtered using fastp (https://github.com/OpenGene/fastp). Clean reads were mapped to the Nipponbare genome (MSU v7.0, http://rice.uga.edu/) using BWA (version 0.7.10-r789) (Li & Durbin, 2009) with default parameters. The duplicates were removed using the Mark Duplicate function of Picard, and InDel-based realignment and base recalibration were performed using GATK (McKenna et al., 2010).

GATK was used for the variant calling of SNPs and InDels in all RILs, and the following SNPs were strictly filtered: two SNPs within 5 bp; SNPs within 5 bp near InDels; and two InDels at <10 bp (Reumers et al., 2012). The SNPs were selected based on the following restrictions: (i) the SNP genotypes of the parents were homozygous for different alleles; (ii) the depth of the SNPs in the parents was greater than 10×; and (iii) the SNPs were located on a chromosome. All filtered SNPs were used to divide the bin blocks with the sliding window method (15 SNPs formed a sliding window, and 1 SNP constituted a step) (Huang et al., 2009). Finally, a bin-based genetic map was generated using HighMap (Liu et al., 2014).

Investigation and QTL mapping of PH-related traits

Fifteen days before the rice harvest, the plants from Luohui 9, RPY geng, RILs, YTB, Z7B, and testcross F_1 were sampled. To preclude border effects, no less than 15 plants from the middle of each RIL or cross line (6 × 10 plants) plot were randomly sampled for investigating PH and TN, and only the main panicle of each plant was used to measure PH, PL, D1, D2, and D3. In each season, the average of the measured plants in each plot was used for subsequent QTL mapping. In total, PH was investigated in HN162, HB171, HB181, HN182, and HB191. PL was investigated in HN162, HB171, HB181, and HN182. TN was recorded in HN162 and HB181. To decipher PH in detail, PH in HN182 was divided into PL and three ILs (D1, D2, and D3) for QTL analysis (Figure S3b).

Based on the bin-based genetic map, the QTL mapping of PH, PL, D1, D2, D3, and TN was performed using the composite interval mapping (CIM) method with the R package 'Rqtl' (Arends et al., 2010). The threshold was set to 1000 times the PT test, and a

significance level of 0.1 was considered the critical value for QTL significance. The confidence interval was calculated using the 'lodint' function (Dupuis & Siegmund, 1999), and the drop value was set to 1.5. MapChart was used to visualize the distribution of all identified QTLs on 12 chromosomes (Voorrips, 2002).

QTL mapping of heterosis-related loci

For the mapping of heterosis-related loci, the GCA, MPH, and BPH values were calculated in two testcross populations as follows:

$$\mathrm{GCA} = \overline{yi.} - \overline{y..},$$

where $\overline{yi.}$ is the average PH of each hybrid combination and $\overline{y..}$ is the average PH of all offspring. Moreover,

$$\mathrm{MPH} = (F_1 - \mathrm{MP})/\mathrm{MP} \times 100\%,$$

$$\mathrm{BPH} = (F_1 - \mathrm{BP})/\mathrm{BP} \times 100\%,$$

where F_1 is the average PH of the hybrid F_1 generation, MP is the average PH of the parents, and BP is the higher value from the parents.

The QTLs for GCA, MPH, and BPH were analyzed using the CIM method with the R package 'Rqtl'. The LOD value was 2.5, and the confidence interval was determined using the 'lodint' function at a drop value of 1.5.

Analysis of the genetic effects of *qPH-3.1* and *qPH-5.1*

According to the bin alleles of QTLs, the genetic effects of *qPH-3.1* and *qPH5-5.1* were analyzed through hybrid experiments between two opposite-allele RILs in which the alleles of the other PH-related QTLs were the same to minimize background effects (Li et al., 2015). In addition, the two RILs have high genome-wide level background consistency (>60%) and similar flowering periods to facilitate the crossing.

Vector construction, rice transformation, and growth conditions

To generate *qph-3.1* and *qph-5.1* mutants, two single guide RNAs (sgRNAs) targeting two different positions of the *qPH-3.1* and *qPH-5.1* genes were designed and cloned into a CRISPR–Cas9 vector. *Agrobacterium tumefaciens*-mediated *transformation was performed in rice (japonica*, Zhonghua11) (BioRun, Wuhan, China). All primers used to construct the vectors and confirm the edit results are listed in Table S10.

Three independent homozygous CRISPR–Cas9 mutation lines of the T_3 generation were used for gene function analysis of each gene. The control plants and independent transgenic lines were grown in a paddy field at Wuhan University (30°N, 114°E) under natural conditions in the summer of 2021. Field management was performed with standard procedures during the growth period. Phenotypic data were collected at the maturing stage.

ACKNOWLEDGMENTS

The National Key Research and Development Program of China (2016YFD0100400) and the National Special Key Project for Transgenic Breeding (grant No. 2016ZX08001001) funded this study. We thank Professor Qian Qian (State Key Laboratory of Rice Biology, China National Rice Research Institute, Hangzhou, Zhejiang, 310 006, People's Republic of China) for proving us RPY geng materials. We thank Professor Zhang Xiaoming (Institute for Crop and Nuclear Technology Utilization, Zhejiang Academy of Agricultural Sciences, Hangzhou, Zhejiang, 310 021, People's Republic of China) for giving us the Z7A cytoplasmic male sterile line. We are grateful to Professor Liu Shengyi (Chinese Academy of Agricultural Sciences, Ministry of Agriculture & Rural Affairs, Key Laboratory of Biology & Genetic Improvement of Oil Crops, Oil Crops Research Institute, Wuhan 430 062, People's Republic of China) for providing us with valuable comments during writing. The authors also thank the anonymous referees, whose constructive comments were helpful in improving the quality of this work.

CONFLICT OF INTEREST

The authors declare that they have no competing interests.

DATA AVAILABILITY STATEMENT

All resequencing datasets of RILs have been deposited in the Sequence Read Archive (SRA) database of the NCBI under accession number PRJNA803765.

SUPPORTING INFORMATION

Additional Supporting Information may be found in the online version of this article.

Figure S1. Luohui 9–RPY geng hybrid F_1 plants.

Figure S2. Flowchart of the experimental design and analysis procedure used in this study.

Figure S3. Schematic diagram of planting environment (a) and measurement methods of plant height-related traits (plant height, panicle length, internode length) (b).

Figure S4. Venn diagram of known genes related to plant height, tiller number, internode length, and panicle length.

Figure S5. Multiple alleles of the *sd1* gene (a) and nucleotide (b) and amino acid (c) sequence alignments of sd1 between RPY geng, Luohui 9, and Nipponbare.

Figure S6. The *OsCICR* gene location (a) and comparison of plant height (b), internode length (c), panicle length (d), tiller number (e), and number of grains per panicle (f) between the parent allele RILs.

Figure S7. Comparison of plant height (a, b) and internode length (c, d) of RILs of parent alleles of the *Ostrxm* gene block, without considering the influence of the *sd1* allele (a, c) and the background of the Luohui 9 *sd1* allele (b, d).

Figure S8. The *PSRK2* gene location (a) and a comparison of plant height (b), internode length (c), panicle length (d), tiller number (e), and number of grains per panicle (f) of the RILs of the parent alleles of the *PSRK2* gene block.

Figure S9. The *SBI* and *OsCOLE1* gene locations (a, d) and a comparison of plant height (b) and internode length (c, e) of different allele RILs.

Figure S10. Candidate gene positions (a) and number statistics (b) in QTLs.

Figure S11. Plant height (a), internode length (b), and panicle length (c) of different alleles of *qPH-3.1* (the background influence of *sd1* is not considered); plant height (d), internode length (e), and panicle length (f) of different alleles of *qPH-3.1* under the background of the Luohui 9 *sd1* allele. $*P < 0.05$, $**P < 0.01$, $***P < 0.001$, Student's *t*-test. *qPH-3.1Fa* represents the RPY geng allele, *qPH-3.1Mo* represents the Luohui 9 allele.

Figure S12. Candidate gene position of *qPH-5.1* (a) and plant height (b) and internode length (c) of plants with different alleles.

Figure S13. Gene expression profile of the *LOC_Os05g45180* gene.

Figure S14. The position of the candidate gene in *qPH-11.1* (a) and plant height (b, e), panicle length (c, f), and internode length (d, g) of plants with different alleles.

Figure S15. The position of the candidate gene in *qPL-1.4* (a) and plant height (b), internode length (c), panicle length (d), tiller numbers (e), and number of grains per panicle (f), as well as the heatmap of *LOC_Os01g64590* in 39 tissues (g).

Figure S16. The positions of candidate genes in *qTN-5.1* (a, block 145240; f, block 145351) and the tiller number (b, g), plant height (c, h), internode length (d, i), and number of grains per panicle (e, j) of plants with different alleles.

Figure S17. The mutant lines of *qph-3.1* and *qph-5.1*.

Figure S18. QTL of plant height-related traits and heterosis locus of plant height.

Table S1. Statistical analysis results of all plant height-related traits.

Table S2. Details of QTLs for all traits.

Table S3. Summary of published genes for plant height, internode length, panicle length, and tiller number.

Table S4. Summary of the known genes in QTLs.

Table S5. Sequence alignment results of parental protein sequences of seven known genes in QTLs.

Table S6. Summary information of homologs of published genes in QTLs.

Table S7. Genotypes of RILs used for dominance effect analysis in Figure 6.

Table S8. Aggregation types of identified plant height QTL genes.

Table S9. The average plant height of RILs in different combinations of five QTLs.

Table S10. SgRNA target sites and primers of *qPH-3.1* and *qPH-5.1*.

OPEN RESEARCH BADGES

This article has earned an Open Data badge for making publicly available the digitally shareable data necessary to reproduce the reported results. The data are available at: 'Second-generation Illumina data of *indica–japonica* derived recombinant inbred line populations' (https://www.ncbi.nlm.nih.gov/bioproject/PRJNA803765).

REFERENCES

Angira, B., Addison, C.K., Cerioli, T., Rebong, D.B., Wang, D.R., Pumplin, N. et al. (2019) Haplotype characterization of the *sd1* semidwarf gene in United States rice. *Plant Genome*, **12**, 9.

Arends, D., Prins, P., Jansen, R.C. & Broman, K.W. (2010) R/QTL: high-throughput multiple QTL mapping. *Bioinformatics*, **26**, 2990–2992.

Ashikari, M., Sasaki, A., Ueguchi-Tanaka, M., Itoh, H., Nishimura, A., Datta, S. et al. (2002) Loss-of-function of a rice gibberellin biosynthetic gene, *GA20 oxidase* (*GA20ox-2*), led to the rice 'Green Revolution'. *Breeding Science*, **52**, 143–150.

Attitalla, I.H. (2011) Modified CTAB method for high quality genomic DNA extraction from medicinal plants. *Pakistan Journal of Biological Sciences*, **14**, 998–999.

Birchler, J.A., Yao, H., Chudalayandi, S., Vaiman, D. & Veitia, R.A. (2010) Heterosis. *The Plant Cell*, **22**, 2105–2112.

Biswas, S., Tian, J.Q., Li, R., Chen, X.F., Luo, Z.J., Chen, M.J. et al. (2020) Investigation of CRISPR/Cas9-induced *SD1* rice mutants highlights the importance of molecular characterization in plant molecular breeding. *Journal of Genetics and Genomics*, **47**, 273–280.

Dupuis, J. & Siegmund, D. (1999) Statistical methods for mapping quantitative trait loci from a dense set of markers. *Genetics*, **151**, 373–386.

Fan, F.F., Long, W.X., Liu, M.M., Yuan, H.R., Pan, G.J., Li, N.W. et al. (2019) Quantitative trait locus mapping of the combining ability for yield-related traits in wild rice *Oryza longistaminata*. *Journal of Agricultural and Food Chemistry*, **67**, 8766–8772.

Fang, J., Yuan, S., Li, C., Jiang, D., Zhao, L., Peng, L. et al. (2018) Reduction of ATPase activity in the rice kinesin protein Stemless Dwarf 1 inhibits cell division and organ development. *The Plant Journal*, **96**, 620–634.

Fumio, T.S., Yasushi, K., Hiroshi, K., Haruko, O., Akemi, T., Naho, H. et al. (2011) A loss-of-function mutation of rice DENSE PANICLE 1 causes semi-dwarfness and slightly increased number of spikelets. *Breeding Science*, **61**, 17–25.

Hedden, P. (2003) The genes of the green revolution. *Trends in Genetics*, **19**, 5–9.

Huang, X.H., Feng, Q., Qian, Q., Zhao, Q., Wang, L., Wang, A.H. et al. (2009) High-throughput genotyping by whole-genome resequencing. *Genome Research*, **19**, 1068–1076.

Huang, X.H., Kurata, N., Wei, X.H., Wang, Z.X., Wang, A., Zhao, Q. et al. (2012) A map of rice genome variation reveals the origin of cultivated rice. *Nature*, **490**, 497–501.

Janoria, M.P. (1989) A basic plant ideotype for rice. *International Rice Research Newsletter*, **14**, 12–13.

Khush, G.S. (1990) Varietal needs for different environments and breeding strategies. In: Muralidharan, K. & Siddiq, E.A. (Eds.) *New frontiers in rice research*. Hyderabad: Research D.o.R.

Kuroh, T., Nagai, K., Gamuyao, R., Wang, D.R., Furuta, T., Nakamori, M. et al. (2018) Ethylene-gibberellin signaling underlies adaptation of rice to periodic flooding. *Science*, **361**, 181–185.

Li, D.Y., Huang, Z.Y., Song, S.H., Xin, Y.Y., Mao, D.H., Lv, Q.M. et al. (2016) Integrated analysis of phenome, genome, and transcriptome of hybrid rice uncovered multiple heterosis-related loci for yield increase. *Proceedings of the National Academy of Sciences of the United States of America*, **113**, E6026–E6035.

Li, H. & Durbin, R. (2009) Fast and accurate short read alignment with burrows-wheeler transform. *Bioinformatics*, **25**, 1754–1760.

Li, J.A., Jiang, J.F., Qian, Q.A., Xu, Y.Y., Zhang, C., Xiao, J. et al. (2011) Mutation of rice BC12/GDD1, which encodes a kinesin-like protein that binds to a GA biosynthesis gene promoter, leads to dwarfism with impaired cell elongation. *Plant Cell*, **23**, 628–640.

Li, S.C., Xie, K.L., Li, W.B., Zou, T., Ren, Y., Wang, S.Q. et al. (2012) Re-sequencing and genetic variation identification of a rice line with ideal plant architecture. *Rice*, **5**, 7.

Li, X., Li, X.R., Fridman, E., Tesso, T.T. & Yu, J.M. (2015) Dissecting repulsion linkage in the dwarfing gene Dw3 region for sorghum plant height provides insights into heterosis. *Proceedings of the National Academy of Sciences of the United States of America*, **112**, 11823–11828.

Li, X.K., Wu, L., Wang, J.H., Sun, J., Xia, X.H., Geng, X. et al. (2018) Genome sequencing of rice subspecies and genetic analysis of recombinant lines reveals regional yield- and quality-associated loci. *BMC Biology*, **16**, 12.

Liu, D.Y., Ma, C.X., Hong, W.G., Huang, L., Liu, M., Liu, H. et al. (2014) Construction and analysis of high-density linkage map using high-throughput sequencing data. *PLoS One*, **9**, 9.

Liu, F., Wang, P.D., Zhang, X.B., Li, X.F., Yan, X.H., Fu, D.H. et al. (2018) The genetic and molecular basis of crop height based on a rice model. *Planta*, **247**, 1–26.

Mahesh, H.B., Shirke, M.D., Singh, S., Rajamani, A., Hittalmani, S., Wang, G.L. et al. (2016) *Indica* rice genome assembly, annotation and mining of blast disease resistance genes. *BMC Genomics*, **17**, 12.

McKenna, A., Hanna, M., Banks, E., Sivachenko, A., Cibulskis, K., Kernytsky, A. et al. (2010) The genome analysis toolkit: a MapReduce framework for analyzing next-generation DNA sequencing data. *Genome Research*, **20**, 1297–1303.

Peng, S.K.,.G.S. & Cassman, K.G. (1994) Chapter 2: Evolution of the new plant ideotype for increased yield potential. In: Cassman, K.G. (Ed.) *Breaking the yield barrier: proceedings of a workshop on rice yield potential in favorable environments*. Los Baños: Institute, I.R.R.

Reumers, J., De Rijk, P., Zhao, H., Liekens, A., Smeets, D., Cleary, J. et al. (2012) Optimized filtering reduces the error rate in detecting genomic variants by short-read sequencing. *Nature Biotechnology*, **30**, 61–U103.

Sazuka, T., Aichi, I., Kawai, T., Kitano, H. & Matsuoka, M. (2005) The rice mutant dwarf bamboo shoot 1: a leaky mutant of the *NACK-type kinesin-like* gene can initiate organ primordia but not organ development. *Plant and Cell Physiology*, **46**(12), 1934–1943.

Schatz, M.C., Maron, L.G., Stein, J.C., Wences, A.H., Gurtowski, J., Biggers, E. et al. (2014) Whole genome de novo assemblies of three divergent strains of rice, *Oryza sativa*, document novel gene space of *aus* and *indica*. *Genome Biology*, **15**, 16.

Song, J.M., Xie, W.Z., Wang, S., Guo, Y.X., Koo, D.H., Kudrna, D. et al. (2021) Two gap-free reference genomes and a global view of the centromere architecture in rice. *Molecular Plant*, **14**, 1757–1767.

Spielmeyer, W., Ellis, M.H. & Chandler, P.M. (2002) Semidwarf (*sd-1*), "green revolution" rice, contains a defective gibberellin 20-oxidase gene. *Proceedings of the National Academy of Sciences of the United States of America*, **99**, 9043–9048.

Springer, N. (2010) Shaping a better rice plant. *Nature Genetics*, **42**, 475–476.

Su, S., Hong, J., Chen, X.F., Zhang, C.Q., Chen, M.J., Luo, Z.J. et al. (2021) Gibberellins orchestrate panicle architecture mediated by DELLA-KNOX signalling in rice. *Plant Biotechnology Journal*, **19**, 2304–2318.

Virmani, S.S. (1994) Prospects of hybrid rice in the tropics and subtropics. In: Virnani, S.S. (Ed.) *Hybrid rice technology: new developments and future prospects*. Manila: International Rice Research Institute, pp. 7–19.

Voorrips, R.E. (2002) MapChart: software for the graphical presentation of linkage maps and QTLs. *The Journal of Heredity*, **93**, 77–78.

Wang, S.S., Wu, K., Qian, Q., Liu, Q., Li, Q., Pan, Y.J. et al. (2017) Non-canonical regulation of SPL transcription factors by a human OTUB1-like deubiquitinase defines a new plant type rice associated with higher grain yield. *Cell Research*, **27**, 1142–1156.

Wang, W., Mauleon, R., Hu, Z., Chebotarov, D. & Leung, H. (2018) Genomic variation in 3,010 diverse accessions of Asian cultivated rice. *Nature*, **557**, 43–49.

Xiang, C., Zhang, H.J., Wang, H., Wang, J., Wang, W.S., Xia, J.F. et al. (2016) Dissection of combining ability for yield and related traits using introgression lines in the background of a key restorer line in rice (*Oryza sativa* L.). *Field Crops Research*, **193**, 154–163.

Xu, S.Z., Xu, Y., Gong, L. & Zhang, Q.F. (2016) Metabolomic prediction of yield in hybrid rice. *The Plant Journal*, **88**, 219–227.

Yu, H.P., Ren, D.Y., Zhu, Y.Z., Xu, J.M., Wang, Y.X., Liu, R.F. et al. (2016) *MULTI-TILLERING DWARF1*, a new allele of *BRITTLE CULM 12*, affects plant height and tiller in rice. *Scientific Bulletin*, **61**, 1810–1817.

Yu, Y.L., Hu, X.J., Zhu, Y.X. & Mao, D.H. (2020) Re-evaluation of the rice 'Green Revolution' gene: the weak allele *SD1-EQ* from *japonica* rice may be beneficial for super *indica* rice breeding in the post-green revolution era. *Molecular Breeding*, **40**, 12.

Yuan, L.P. (1994) Increasing yield potential in rice by exploitation of heterosis. In: Virnani, S.S. (Ed.) *Hybrid rice technology: new developments and future prospects*. Manila: International Rice Research Institute, pp. 1–6.

Yuan, L.P. & Virnani, S.S. (1988) Status of hybrid rice research and development. In: Virnani, S.S. (Ed.) *Hybrid rice. Proceedings of the international symposium on hybrid rice*. Changsha: International Rice Research Institute, pp. 7–24.

Zhang, G.Q. (2020) Prospects of utilization of inter-subspecific heterosis between *indica* and *japonica* rice. *Journal of Integrative Agriculture*, **19**, 1–10.

Zhang, M., Zhang, B.C., Qian, Q.A., Yu, Y.C., Li, R., Zhang, J.W. et al. (2010) Brittle Culm 12, a dual-targeting kinesin-4 protein, controls cell-cycle progression and wall properties in rice. *The Plant Journal*, **63**, 312–328.

Zhou, H., Xia, D., Zeng, J., Jiang, G.H. & He, Y.Q. (2017) Dissecting combining ability effect in a rice NCII-III population provides insights into heterosis in *indica-japonica* cross. *Rice*, **10**, 9.